

RESEARCH ARTICLE

DRUG DEVELOPMENT RESEARCH

WILEY

Discovery of novel indole-1,2,4-triazole derivatives as tubulin polymerization inhibitors

Meng-Ke Wu¹ | Ruo-Jun Man¹  | Yan-Juan Liao¹ | Hai-Liang Zhu² | Zhu-Gui Zhou³

¹Guangxi Biological Polysaccharide Separation, Purification and Modification Research Platform, Guangxi University for Nationalities, Nanning, China

²State Key Laboratory of Pharmaceutical Biotechnology, Nanjing University, Nanjing, China

³College of Chemistry and Chemical Engineering, Guangxi Key Laboratory of Polysaccharide Materials and Modifications, Guangxi University for Nationalities, Nanning, China

Correspondence

Ruo-Jun Man, Guangxi Biological Polysaccharide Separation, Purification and Modification Research Platform, Guangxi University for Nationalities, Nanning 530006, China.
Email: manruojun@163.com

Hai-Liang Zhu, State Key Laboratory of Pharmaceutical Biotechnology, Nanjing University, Nanjing 210023, China.
Email: zhuhl@nju.edu.cn

Zhu-Gui Zhou, College of Chemistry and Chemical Engineering, Guangxi Key Laboratory of Polysaccharide Materials and Modifications, Guangxi University for Nationalities, Nanning, 530006, China.
Email: zhouzhugui@126.com

Funding information

Guangxi Biological Polysaccharide Separation, Purification and Modification Research Platform, Grant/Award Number: GKZY18076005; Guangxi Natural Science Foundation, Grant/Award Number: 2019AC20294; Guangxi University for Nationalities Research Funded Project, Grant/Award Number: 2018KJQD13; Lianyungang Talent Project

Abstract

A series of novel indole-1,2,4-triazole derivatives have been designed, synthesized, and evaluated as potential tubulin polymerization inhibitors. The top hit **12**, bearing the 3,4,5-trimethoxyphenyl moiety, exhibited substantial anti-proliferative activity against HepG2, HeLa, MCF-7, and A549 cells in vitro with IC₅₀ values of 0.23 ± 0.08 μM, 0.15 ± 0.18 μM, 0.38 ± 0.12 μM, and 0.30 ± 0.13 μM, respectively. It also inhibited tubulin polymerization with the IC₅₀ value of 2.1 ± 0.12 μM, which was comparable with that of the positive controls. Furthermore, compound **12** regulated the expression of cell cycle-related proteins (Cyclin B1, Cdc25c, and Cdc2) and apoptosis-related proteins (Bcl-2, Bcl-x, and Mcl-1). Mechanistically, compound **12** could arrest cell cycle at the G2/M phase, thus induce an increase of apoptotic cell death. In addition, molecular docking hinted the possible interaction mode of compound **12** into the colchicine binding site of tubulin heterodimers. According to the applications of microtubule-targeting agents in both direct and synergistic cancer therapies, we hope this work might be of significance for future researches.

KEYWORDS

colchicine-binding site, indole-1,2,4-triazole, microtubules, molecular docking

1 | INTRODUCTION

In the past decades, the reported natural and synthetic compounds targeting the mitotic spindle apparatus have attracted wide attention, and microtubules (MTs) have been recognized as a crucial target for the development of potential novel anticancer agents (Mahindroo et al., 2006). Currently, the drugs, which can bind to specific target or multitargets with the characteristics of high-efficiency and low

toxicity, are preferred over traditional cytotoxic treatment. Among them, microtubule-targeting agents (MTAs) are a major advancement in the treatment of a considerable fraction of cancers in the pharmacy field (Meng et al., 2009). MTs are cytoskeleton protein polymers composed of α,β-tubulin heterodimers that are vital components in eukaryotic cells (Amos, 2004; Dumontet & Jordan, 2010; Jordan & Wilson, 2004; Kavallaris et al., 2001; Risinger et al., 2009). They play an essential role in the process of cells division, cell shape formation, maintenance, cell signaling, cell transport of organelles, as well as the secretion, regulation of motility, and segregation of chromosomes

Meng-Ke Wu and Ruo-Jun Man contributed equally to the work

(McIntosh et al., 2002; Walczak, 2000). Upon breaking down the balance between tubulin polymerization and depolymerization, MTs function will be interfered, interrupting the cell division and encouraging the apoptosis (Honore et al., 2005; Teicher, 2008; Nakagawa-Goto et al., 2011). Therefore, MTs have become an attractive target for the exploitation of novel chemotherapeutic drugs and therapies (Brennan et al., 2013; Gan et al., 2013).

The design of targeting drugs is a popular field. A lot of modified compounds which can bind to tubulin have been reported. Because of the effective interference with microtubule polymerization, colchicine (compound **1**, Figure 1) has been identified a potentially useful anticancer drug, and its binding site on tubulin has been characterized already (Nakagawa-Goto et al., 2011; Ravelli et al., 2004). However, due to the high adverse effect, the clinical development of colchicine for cancer treatment was not successful (Zhou & Giannakakou, 2005). Among the natural compounds, combretastatins could affect microtubule dynamics by binding to the colchicine site (Sharma et al., 2010). Combretastatin A-4 (CA-4, **2a**, Figure 1) exhibited strong growth inhibition at nanomolar concentrations against a wide variety of human cancers including multidrug resistant (MDR) types (Flynn et al., 2011). Low water solubility of CA-4 limited its efficacy in vivo, hence, water soluble combretastatin analogs have been further developed (Yu et al., 2015). Combretastatin A-4P (CA-4P, **2b**, Figure 1), a water-soluble disodium phosphate derivative, has shown promising results in human clinical trials. CA-4P is under evaluation in phase III trials for the treatment of anaplastic thyroid cancer and in phase II trials for non-small-cell lung cancer and platinum-resistant ovarian cancer (Rustin et al., 2010; Zweifel et al., 2011). With no commercialized cases but great potential in direct or

synergistic therapies for treating cancers, developing anti-tubulin agents remains a challenge.

Previous studies have yielded numerous small molecule compounds with different heterocycles such as piperazine, imidazoles, thiazole, indoles, pyrazoline, and oxadiazole (Kamal, Kumar, et al., 2014a; Kamal, Reddy, et al., 2014b; Szczepankiewicz et al., 2001). These synthetic compounds were potent in the inhibition of tubulin polymerization. In particular, indole analogues (**3** and **4**, Figure 1) have been identified to possess potent antitumor and tubulin depolymerization activity (Tanitame et al., 2004). Moreover, 1,2,4-triazole analogues have also been a common choice in potent tubulin polymerization inhibitors (**5**, Figure 1) (Alhamadsheh et al., 2007; Campbell & Cronan, 2001; Li, Li, et al., 2011b; Li, Luo, & Zhu, 2011a).

Structure activity relationship (SAR) studies of colchicine and CA-4 (CA-4P) revealed that the 3,4,5-trimethoxy phenyl ring was essential for activity (Pettit et al., 2000; Pettit & Rhodes, 1998; Solum et al., 2014). Similar compounds were designed and synthesized. Due to their performances at the colchicine binding site on tubulin, these compounds with identical skeleton could inhibit tubulin polymerization well and exhibit potent antitumor activity in vivo against various tumors. According to the molecular modeling studies and the results of previous researches, we attempted to integrate these two groups to screen new basic scaffolds for the design of a series of novel tubulin assembling inhibitors (**7-24**, Figure 1). As the designing strategy, we started the investigation by using the indole-containing backbone, and set the 3,4,5-trimethoxyphenyl moiety as one choice of the substitutes.

Here, we searched more novel agents to extend our research and gain further insight into the ensuing structure-activity relationships

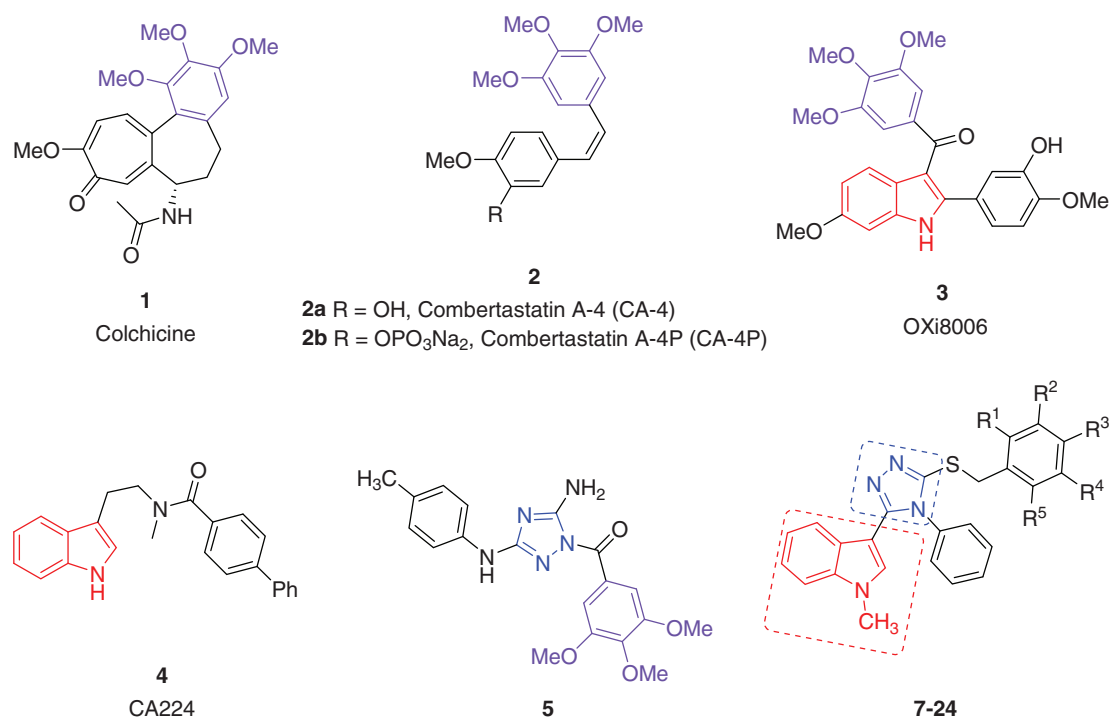


FIGURE 1 Chemical structures of known tubulin inhibitors and designed structures

(SARs). Our screening strategy was to perform modifications on the aromatic ring to find the one with the best inhibitory activity. In this work, we synthesized a series of tubulin inhibitors bearing indole-1,2,4-triazole scaffold and emphasized the rationale behind the discovery of inhibitors, the discussion of synthetic method, SAR, bioactivities, and the effect of the inhibitors on the viability of tumor cells.

2 | RESULTS AND DISCUSSION

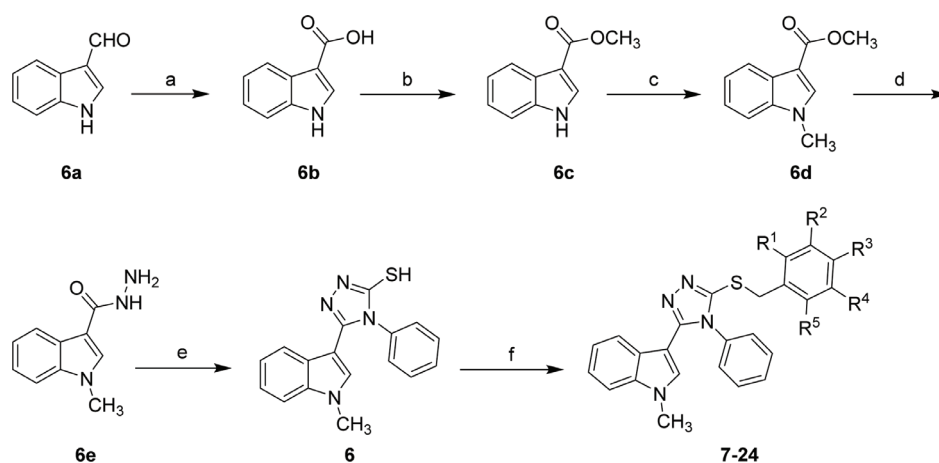
2.1 | Chemistry

As illustrated in Scheme 1, 19 novel indole-1,2,4-triazole derivatives were synthesized via the general pathway. They were obtained in six steps and started from indole-3-carboxaldehyde (**6a**) in acetone, KMnO_4 was added and the reaction was heated for 5–6 h. The obtained compound **6b** was dissolved in MeOH, then H_2SO_4 was added softly, and the reaction was refluxed to gain compound **6c**. Compound **6c** was further treated with

iodomethane to yield compound **6d**, with sodium hydride as catalyst. The hydrazides (compound **6e**) were obtained from the reaction of esters **6d** and 85% hydrazine hydrate in ethanediol. Treatment of the hydrazide with phenyl isothiocyanate under refluxing gave the key intermediate **6**. After dissolving in acetonitrile, compound **6** was reacted with different substituted benzyl bromide to afford the target compounds **7–24**. All of the target compounds (Table 1) gave satisfactory analytical and spectroscopic data, which were in full accordance with their assigned structures.

2.2 | Anti-proliferation assay

All the synthesized compounds **6–24** were evaluated for their in vitro anti-proliferation activity against HepG2 (human hepatoma cells), HeLa (human cervix cell), MCF-7 (human breast cancer cell), and A549 (human lung cancer cell). All of the chosen tumor cell lines were typical ones associated with the polymerization of tubulin. As reported in Table 1, the results indicated that the top hit **12** exhibited appreciable antiproliferative effect, especially for HeLa cells. Compared with



Compounds	R ¹	R ²	R ³	R ⁴	R ⁵
7	H	H	H	H	H
8	F	H	H	H	F
9	H	Cl	F	H	H
10	H	H	OCH ₃	H	H
11	H	OCH ₃	H	OCH ₃	H
12	H	OCH ₃	OCH ₃	OCH ₃	H
13	F	H	H	H	H
14	Cl	H	H	H	H
15	Br	H	H	H	H
16	H	F	H	H	H
17	H	Cl	H	H	H
18	H	Br	H	H	H
19	H	H	F	H	H
20	H	H	Cl	H	H
21	H	H	Br	H	H
22	H	H	I	H	H
23	H	H	CH ₃	H	H
24	H	H	CF ₃	H	H

SCHEME 1 General synthesis and structures of compounds (**7–24**). Reagents and conditions: (a) KMnO_4 , acetone, reflux, 5–6 h; (b) H_2SO_4 , methanol, 80°C, 8–11 h; (c) CH_3I , NaH, THF, 35°C; (d) hydrazine hydrate (85%), ethanediol, 180°C, 6 h; (e) phenyl isothiocyanate, ethyl alcohol, 80°C, 4–6 h; (f) substituted benzyl bromide, acetonitrile, 90°C, 12 h

TABLE 1 The substitutes of the synthesized compounds.

Compounds	R ¹	R ²	R ³	R ⁴	R ⁵
7	H	H	H	H	H
8	F	H	H	H	F
9	H	Cl	F	H	H
10	H	H	OCH ₃	H	H
11	H	OCH ₃	H	OCH ₃	H
12	H	OCH ₃	OCH ₃	OCH ₃	H
13	F	H	H	H	H
14	Cl	H	H	H	H
15	Br	H	H	H	H
16	H	F	H	H	H
17	H	Cl	H	H	H
18	H	Br	H	H	H
19	H	H	F	H	H
20	H	H	Cl	H	H
21	H	H	Br	H	H
22	H	H	I	H	H
23	H	H	CH ₃	H	H
24	H	H	CF ₃	H	H

colchicine and ABT-751 as the positive controls, IC₅₀ values of compound **12** were found to be favorable against the four carcinoma cell lines (IC₅₀ = 0.23 ± 0.08 μM, 0.15 ± 0.18 μM, 0.38 ± 0.12 μM, and 0.30 ± 0.13 μM, respectively).

2.3 | Tubulin polymerization inhibition

Since compounds **6–24** were designed for inhibiting tubulin polymerization, we evaluated them on the inhibition of tubulin polymerization *in vitro*. The results were also shown in Table 1. Accordingly, these agents showed inhibitory activities of tubulin and the displayed IC₅₀ values ranged from 2.1 ± 0.12 to 35.79 ± 1.05 μM, as compared with 2.52 ± 0.23 μM of colchicine. Among all the compounds, compound **12** showed the most potent anti-tubulin (IC₅₀ = 2.1 ± 0.12 μM) activity, which was even better than that of the positive controls. Besides, **10** and **11** also appreciably inhibited tubulin polymerization (IC₅₀ = 5.08 ± 0.16, 3.4 ± 0.43 μM), respectively. The correlation coefficient (*R*²) between the tubulin inhibition and the anti-proliferation potency was calculated as 0.7833 (larger than a general 0.4 for checking the positive-correlation). Therefore we could conclude that the synthesized compounds were potential inhibitors of tubulin assembly and the inhibitory effect was roughly proportional with the antiproliferative potency.

2.4 | Cytotoxicity test

All the compounds were evaluated for their toxicity against the non-cancer cell line (human kidney epithelial cell 293T) with the median cytotoxic concentration (CC₅₀) data via the MTT assay. This cell line

was a typical epithelial cell line for evaluation of cytotoxicity. The results shown in Table 2 indicated that most of the obtained compounds had low toxicity upon 293T cells.

2.5 | Structure–activity relationship analysis

Subsequently, SAR were derived from analysis of antiproliferative and tubulin inhibitory activity data. Some general hints could be inferred based on the data. Initially, the phenyl group seemed necessary because compound **6** with a short chain was less potent in all the compounds. If there was no substitution (compound **7**), the phenyl group also showed limited improvement on the activity. Second, the electron-donating groups (–OMe, –Me; compounds **10–12**, **23**) were more favorable than the electron-withdrawing ones (–F, –Cl, –Br, –I, –CF₃; compounds **8**, **9**, **13–22**, **24**). In the electron-donating situation, introducing more such substitutes might enhance the potency; while in the electron-withdrawing situation, especially compounds **13–22**, reducing the size of such substitutes might be beneficial whereas the position seemed a less important parameter. That was to say, although we introduced a variety of substitutes to enrich the diversity by changing the position of the halogen atom from the *ortho*-position to the *meta*-position and *para*-position, the fluoro-substituted ones were more beneficial. Actually, for fluoro-substituted ones, the *ortho*-position was better. Additionally, when the substitutes were electron-withdrawing, introducing multisubstitution (compounds **8**, **9**) could also improve the activity. In brief, the new class of compounds raised several potent tubulin inhibitors, which have the potential to further explore the values of development.

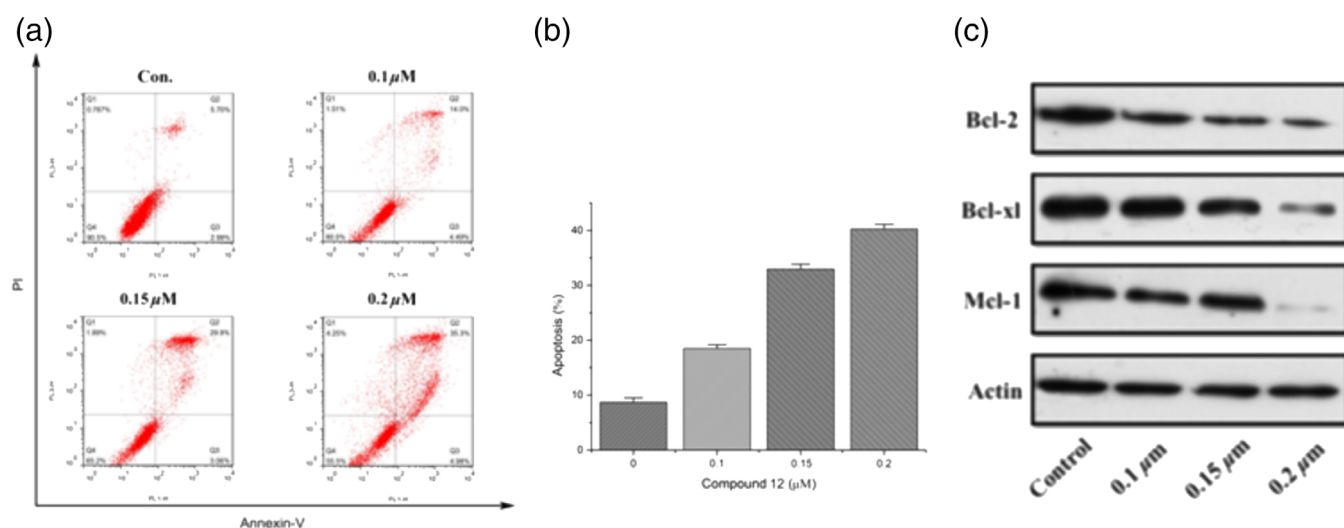
2.6 | Cell apoptosis

To investigate the ability of compound **12** to induce cell death, flow cytometry of cells double stained with Annexin V-FITC/propidium iodide (PI) was conducted. In this study, HeLa cells were treated with compound **12** for 24 h at the concentrations of 0, 0.1, 0.15, and 0.2 μM to examine the apoptotic effect. As shown in Figure 2, the results displayed that the early apoptotic cells were increased from 2.99% to 4.98%. Moreover, the percentage of apoptotic cell significantly increased from 14.0% to 35.3% along with the increasing doses of compound **12**. Thus, compound **12** was efficiently in the induction of apoptosis in a dose-dependent manner.

To further check the compound **12**-induced cell apoptosis, we performed the western blot analysis. It is well-known that regulation of Bcl-2 proteins shares the signaling pathways induced by anti-microtubule compounds. Whereas antiapoptotic members (Bcl-2, Bcl-x1, and Mcl-1) are capable of antagonizing the proapoptotic proteins. In agreement with these observations, we found that the levels of Bcl-2 and Bcl-x1 after 24 h treatment with compound **12** were gradually decreased, while the expression of Mcl-1 (another antiapoptotic member of the Bcl-2 family) was also down-regulated. Altogether, our findings indicated that compound **12** was able to downregulate the

TABLE 2 IC₅₀ values (μM) of the synthesized compounds 6–24 and the positive controls in human tumor cell lines and normal cell line

Compounds	IC ₅₀ ± SD (μM)					CC ₅₀ (μM)
	HepG2 ^a	HeLa ^a	MCF-7 ^a	A549 ^a	Tubulin ^b	293T ^c
6	11.57 ± 0.24	10.34 ± 0.14	13.13 ± 0.17	8.55 ± 0.42	35.79 ± 1.05	105
7	5.58 ± 0.12	3.14 ± 0.31	3.56 ± 0.74	4.14 ± 0.32	23.77 ± 0.64	167
8	1.49 ± 0.06	2.27 ± 0.17	1.46 ± 0.86	1.24 ± 0.37	7.09 ± 0.32	98.7
9	1.56 ± 0.14	1.88 ± 0.08	2.74 ± 0.11	2.86 ± 0.15	8.87 ± 0.98	107
10	0.95 ± 0.09	0.54 ± 0.87	0.78 ± 0.39	0.58 ± 0.31	6.08 ± 0.16	115
11	0.37 ± 0.56	0.38 ± 0.25	0.45 ± 0.18	0.34 ± 0.32	4.40 ± 0.43	136
12	0.23 ± 0.08	0.15 ± 0.18	0.38 ± 0.12	0.30 ± 0.13	2.10 ± 0.12	126
13	1.33 ± 0.05	1.15 ± 0.34	1.48 ± 0.07	1.30 ± 0.11	9.64 ± 0.78	108
14	2.44 ± 0.09	2.63 ± 0.66	2.97 ± 0.12	3.25 ± 0.76	13.45 ± 0.12	142
15	2.84 ± 0.17	1.86 ± 0.32	2.46 ± 0.29	3.87 ± 1.10	15.58 ± 0.34	118
16	2.63 ± 0.14	3.12 ± 0.23	2.73 ± 0.67	2.66 ± 0.56	10.99 ± 0.76	88.9
17	3.04 ± 0.36	2.88 ± 0.14	2.47 ± 0.10	3.38 ± 0.19	14.79 ± 0.22	147
18	2.95 ± 0.45	2.34 ± 0.67	3.78 ± 0.09	2.58 ± 0.23	13.34 ± 0.57	97.6
19	3.58 ± 0.39	2.14 ± 0.76	2.56 ± 0.47	2.14 ± 0.21	11.56 ± 0.30	189
20	2.42 ± 0.04	1.23 ± 0.35	2.46 ± 0.77	2.76 ± 0.81	12.82 ± 0.39	113
21	2.67 ± 0.55	2.12 ± 0.16	2.19 ± 0.29	3.97 ± 0.54	13.67 ± 0.24	157
22	3.76 ± 0.20	2.67 ± 0.17	3.67 ± 0.43	3.26 ± 0.05	19.78 ± 0.67	124
23	0.99 ± 0.35	1.07 ± 0.76	0.86 ± 0.26	0.95 ± 0.28	6.92 ± 0.21	99.6
24	2.08 ± 0.39	1.96 ± 0.22	1.93 ± 0.76	2.87 ± 0.54	12.44 ± 0.76	121
Colchicine ^d	0.35 ± 0.20	0.28 ± 0.11	0.44 ± 0.09	0.37 ± 0.14	2.52 ± 0.23	93.5
ABT-751 ^d	3.82 ± 0.36	0.95 ± 0.08	4.12 ± 0.36	6.10 ± 0.54	8.24 ± 0.69	102

^aInhibition of the growth of tumor cell lines.^bInhibition of tubulin polymerization.^cInhibition of the growth of normal cell line.^dUsed as a positive control.**FIGURE 2** Annexin V-FITC/PI dual-immuno-fluorescence staining after treatment with different concentrations of compound 12 on HeLa cells revealed significantly increased percentage of apoptotic cells. (a) The apoptosis rate of HeLa cells treated with 0, 0.1, 0.15, and 0.2 μM for 24 h. (b) The percentages of apoptotic cells were calculated after the treatment of compound 12. Images were representative of three independent experiments. (c) Western blot analysis of Bcl-2, Bcl-x1, and Mcl-1 after treatment of HeLa cells with compound 12 at the concentrations of 0, 0.1, 0.15, and 0.2 μM for 24 h

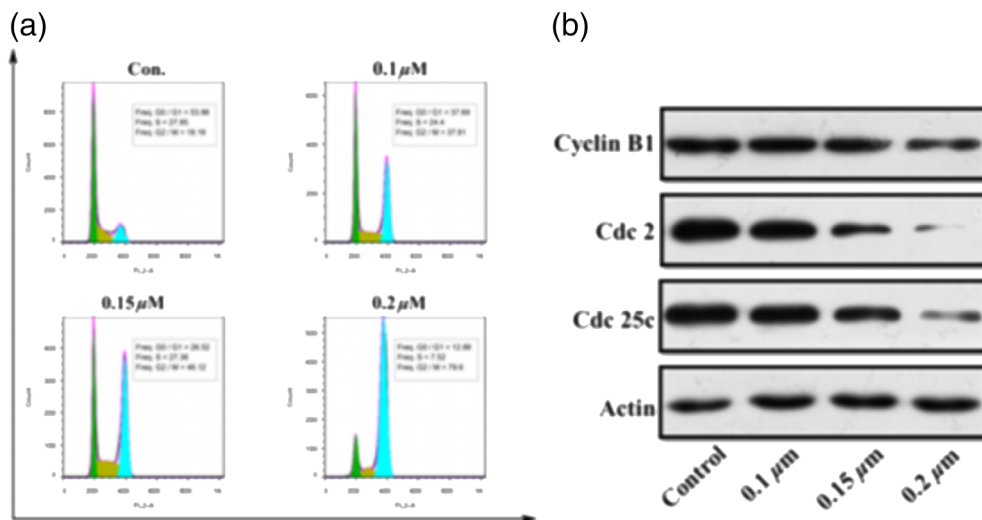


FIGURE 3 (a) Effect of compound **12** on the cell cycle distribution of HeLa cells in a dose-dependent manner (0, 0.1, 0.15, and 0.2 μ M). Images were representative of three independent experiments. (G1 phase, green; S phase, yellow; and G2/M phase, blue). (b) Western blot analysis of the levels of the G2/M-related proteins Cdc2, Cyclin B1, and Cdc25c after treating HeLa cells with compound **12** at the mentioned concentrations for 24 h

expression of antiapoptotic proteins in line, thus effectively to increase the percentage of apoptotic cells.

2.7 | Cell cycle arrest

To further characterize the cell growth inhibitory properties of the new compound **12** on the cell cycle, another flow cytometry assay was carried out. We attempted to confirm whether HeLa cells were blocked in mitosis with G2/M cell cycle arrest. Compound **12** with the various concentrations (0, 0.1, 0.15, and 0.2 μ M) was used on HeLa cells for 24 h. The cells were stained with PI for 30 min. The results of cell cycle profile were subsequently analyzed by flow cytometry. A concomitant decrease in cell population (G1 and S) was detected. As shown in Figure 3, compound **12** caused a rise in G2/M arrest with increased drug concentration. The percentage of cells arrested at the G2/M phases was observed increasing from 18.19% to 37.19%, 46.12%, and 79.6%, respectively.

Then we analyzed the proteins that controlled the cell cycle pathway. Generally speaking, entry into mitosis of eukaryotic cell was regulated by activation of Cdc2 kinase, Cdc25c phosphorylation, and Cyclin B1 binding. As shown in Figure 3, compound **12** caused a dose-dependent decrease in Cdc2, Cdc25c, and Cyclin B1. This result indicated that the arrest at G2/M induced by the compound **12** caused significant variations in Cyclin B1 expression, followed by a remarkable decrease in the level of the phosphorylated forms of both Cdc2 and Cdc25c, especially with the added concentration of 0.2 μ M. The decline in the level of Cdc2 after 24 h was highly significant. The results, which were consistent with the cell cycle analysis, further illustrated the mechanism of the cell cycle arrest effect.

2.8 | Molecular docking

We also visualized the possible binding mode of the colchicine binding site on tubulin from a molecular modeling study for compounds **6–24**. The protein crystal structure of tubulin–colchicine complex was obtained from the Protein Data Bank (PDB code: 4O2B [Prota

et al., 2014]). All docking runs were applied under Discovery Studio 3.5. The interaction energy as the docking calculation of the synthesized compounds ranged from -64.22 to -36.21 kcal/mol. It was clear that compound **12** showed the lowest interaction energy (-64.22 kcal/mol) among all the synthesized compounds. In order to give a better understanding of the tested activity, we examined the interaction mode of the most potent inhibitor **12** within tubulin. For the control colchicine, its trimethoxyphenyl was buried deeply into the β -subunit of tubulin, surrounded by several hydrophobic amino acids, such as Ala, Val, Leu, and Ile (Figure 4(a)). The H-bond of colchicine with Val181 from α -subunit strengthened their interaction with each other. Of course, other kinds of interactions, such as π -alkyl bond, were also helpful. As shown in Figure 4(c) and (d), compound **12** maintained the orientation, especially that of the trimethoxyphenyl motif which mimicked that of colchicine (LOC503). As for the 3,4,5-trimethoxyphenyl moiety, both compound **12** and LOC503 might form one H-bond with Ala250, whereas compound **12** might introduce more H-bonds with Gly237 and Val 238 according to the binding patterns. Moreover, the direction of phenyl from **12** was also similar to the seven-membered ring of LOC503, heading to the gap between tubulin heterodimers. However, π -cation bond between β chain Lys352 and indole ring of **12** was new and different from the H-bond of colchicine. Meanwhile, the numbers of ring contributed more π -interactions, compared with LOC503 (Figure 4(a) and (c)). The 3D interaction mode in Figure 4 revealed that compound **12** was well embedded into the colchicine binding pocket of tubulin dimers and exhibited the most potent affinity for tubulin.

3 | CONCLUSION

A comprehensive series of indole derivatives was developed as a potent cell growth inhibitor, and initial experiments demonstrated that these compounds exhibited significant anticancer activity and tubulin polymerization inhibition activity. We also elucidated SARs between tubulin and the synthesized indole derivatives at colchicine binding site. In summary, compound **12** showed the most potent anticancer

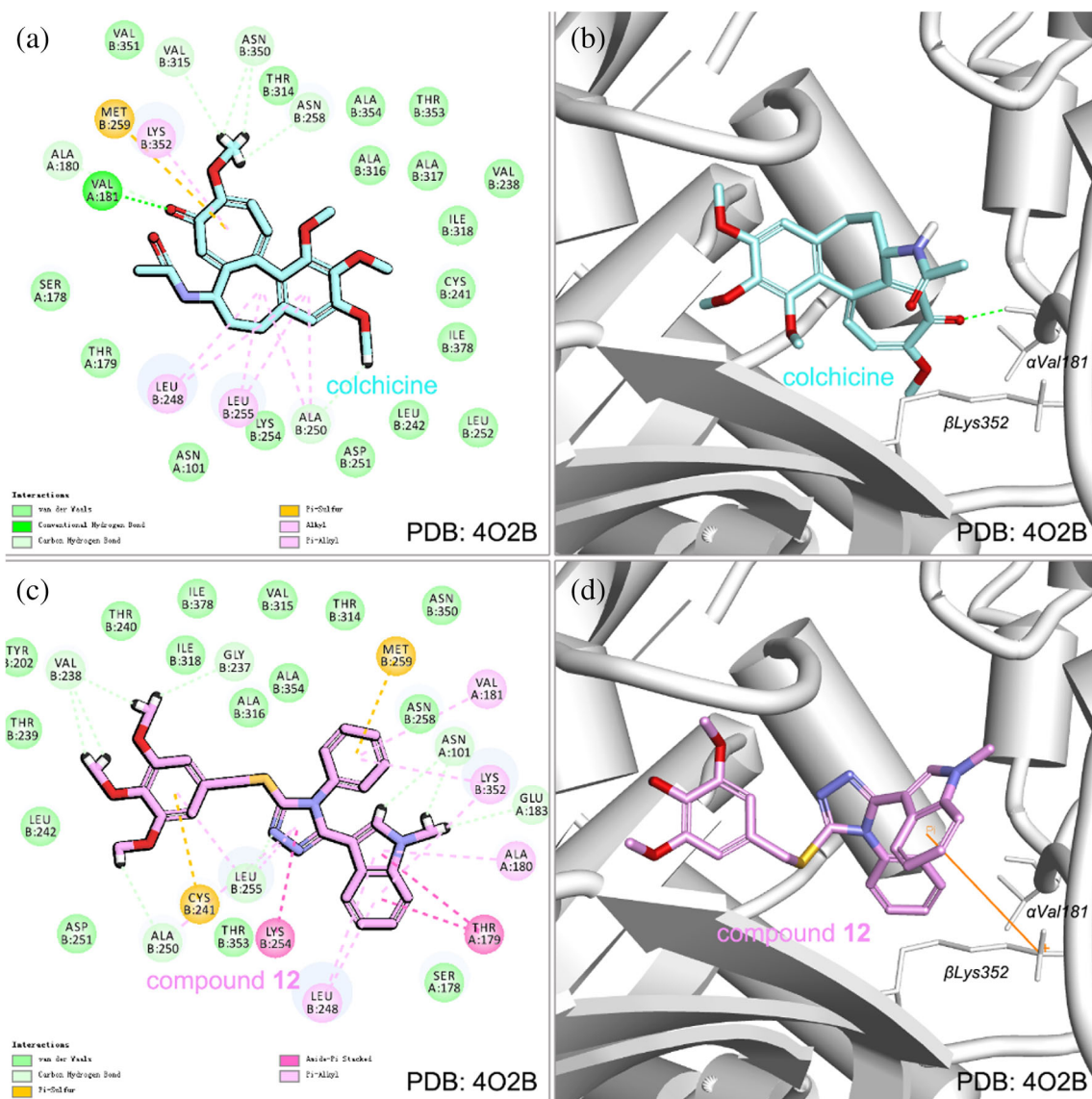


FIGURE 4 Binding mode of compound 12 with the target protein tubulin (PDB code: 4O2B). (a) 2D and (b) 3D diagram of the interaction mode that colchicine with the colchicine binding site. (c) 2D and (d) 3D diagram of the interaction mode that compound 12 with the colchicine binding site

activity against HepG2, HeLa, MCF-7, A549 with IC_{50} values $0.23 \pm 0.08 \mu\text{M}$, $0.15 \pm 0.18 \mu\text{M}$, $0.38 \pm 0.12 \mu\text{M}$, $0.30 \pm 0.13 \mu\text{M}$, and performed impressed tubulin polymerization inhibitory activity with an IC_{50} value of $2.1 \pm 0.12 \mu\text{M}$, which was comparable to that of positive controls. Importantly, the flow cytometry studies demonstrated that compound 12 induced apoptosis in HeLa cells and arrested cells in the G2/M phase of the cell cycle. In order to further study the mechanism, we performed the western blot analysis consulting most microtubule targeting agents. At $0.2 \mu\text{M}$ in HeLa cells, compound 12 induced downregulation of the anti-apoptotic proteins Bcl-2, Bcl-x1, and particularly Mcl-1, which was a key factor governing cell survival. Moreover, compound 12 induced cell cycle arrest at the G2/M phase accompanied with a decrease in mitotic cells. Several key regulators proteins (Cyclin B1, Cdc2, and Cdc25c) coordinated the progress of cells from G2 to M phase. Compound 12 treatment led to a decrease in the level of Cyclin B1 with a concomitant decrease in Cdc2 and

Cdc25c activity. Finally, Molecular docking manifested the inhibitor-tubulin protein interaction and revealed that compound 12 extensively bound to the tubulin at the colchicine binding site. Based on these interesting results of the novel compounds, our work might be served as the starting point as well as provide a reliable approach for reasonable design of tubulin polymerization inhibitors in future.

4 | EXPERIMENTAL SECTION

4.1 | General

All chemicals and reagents used in the current study were of analytical grade. The synthesized compounds were chemically characterized by thin layer chromatography (TLC) on Merck precoated silica GF254 plates and visualized in UV light (254 nm). Melting points (uncorrected)

were determined on a XT4MP apparatus (Taikang Corp., Beijing, China). All the ^1H NMR spectra were recorded on a Bruker DPX 400 model Spectrometer in DMSO-d_6 and chemical shifts were reported in ppm (δ). ESI-MS spectra were recorded on a Mariner System 5304 Mass spectrometer. Elemental analyses were performed on a CHN-O-Rapid instrument and were within $\pm 0.4\%$ of the theoretical values.

4.2 | Chemistry

4.2.1 | General procedure for the preparation of compounds 6b–6d

To a stirred solution of indole-3-carboxaldehyde **6a** (50 mmol) in acetone (100 ml) was added KMnO_4 (10 mmol). The mixture was refluxed under stirring for 5–6 h. The obtained compounds **6b** (40 mmol) in MeOH (100 mL) was added H_2SO_4 (2.9 ml, 40 mmol) dropwise at 0°C . The mixture was further stirred 8–11 h at 80°C . MeOH was evaporated and the pH value was adjusted to 5–6 with aqueous NaHCO_3 . Then the mixture was extracted three times, then organic layer was dried through MgSO_4 and concentrated under reduced pressure. Methyl indole-3-carboxylate **6c** was treated with CH_3I in the presence of NaH in THF at 35°C for 5 h to get products **6d**, respectively. All the reactions were monitored by the thin layer chromatography (TLC).

4.2.2 | General procedure for the preparation of compounds 6e

For the synthesis of substituted compounds **6e** a mixture of corresponding esters **6d** and 85% hydrazine hydrate (1:2) in ethanediol (30 ml) was heated (180°C) to reflux for 6 h. After that, the solution was completely removed under reduced pressure, and the residue crystallized from ethanol.

4.2.3 | General procedure for the preparation of compounds 6

To a solution of the hydrazides **6e** (10 mmol) in ethanol (50 ml) at 80°C , phenyl isothiocyanate (15 mmol) were added, and the reaction mixture was refluxed for 4–6 h. Excess solvent was evaporated under reduced pressure and the residue was dissolved in sodium hydroxide aqueous solution (0.5 h) and then acidified with dilute hydrochloric acid (10%) to pH 5. The precipitate was filtered off, dried, and crystallized from ethanol. In general, compounds **6** was prepared with this method.

4.2.4 | General synthesis method of the target compounds 7–24

Acetonitrile (10 ml) containing compounds **6** (1 mmol) and a variety of benzyl bromide (1.5 mmol) was added to the reaction mixture and

stirred at 90°C until TLC analysis indicated the completion of organic reaction. Then, cool the reaction system to room temperature. The resulting solid was obtained and washed with cold anhydrous ethanol, dried through anhydrous MgSO_4 , and crystallized from anhydrous ethanol to get the pure products.

4.2.5 | 5-(1-Methyl-1H-indol-3-yl)-4-phenyl-4H-1,2,4-triazole-3-thiol (6)

White powder, yield: 82%, m.p. $147\text{--}148^\circ\text{C}$; ^1H NMR (400 MHz, DMSO-d_6) δ : 13.96 (s, 1H), 8.04 (d, $J = 7.9$ Hz, 1H), 7.62 (p, $J = 3.5, 3.0$ Hz, 3H), 7.52–7.41 (m, 3H), 7.27 (dd, $J = 15.3, 1.2$ Hz, 1H), 7.19 (t, $J = 7.5$ Hz, 1H), 6.36 (s, 1H), 3.61 (s, 3H); MS(ESI): 307.1 $[\text{M} + \text{H}]^+$; Anal. Calcd for $\text{C}_{17}\text{H}_{14}\text{N}_4\text{S}$: C 66.64, H 4.61, N 18.29, found: C 66.63, H 4.62, N 18.30.

4.2.6 | 3-(5-[Benzylthio]-4-phenyl-4H-1,2,4-triazol-3-yl)-1-methyl-1H-indole (7)

White powder, yield: 47.7%, m.p. $150\text{--}151^\circ\text{C}$; ^1H NMR (400 MHz, DMSO-d_6) δ : 8.16 (d, $J = 7.8$ Hz, 1H), 7.67–7.53 (m, 4H), 7.46 (d, $J = 8.2$ Hz, 1H), 7.38–7.23 (m, 7H), 7.26–7.15 (m, 1H), 6.49 (s, 1H), 4.37 (s, 2H), 3.62 (m, 3H). MS(ESI): 397.1 $[\text{M} + \text{H}]^+$; Anal. Calcd for $\text{C}_{24}\text{H}_{20}\text{N}_4\text{S}$: C 72.70, H 5.08, N 14.13, found: C 72.71, H 5.09, N 14.11.

4.2.7 | 3-(5-([2,6-Difluorobenzyl]thio)-4-phenyl-4H-1,2,4-triazol-3-yl)-1-methyl-1H-indole (8)

Light yellow powder, yield: 38.4%, m.p. $177\text{--}179^\circ\text{C}$; ^1H NMR (400 MHz, DMSO-d_6) δ : 8.16 (d, $J = 8.0$ Hz, 1H), 7.68–7.55 (m, 4H), 7.51–7.34 (m, 3H), 7.26 (t, $J = 7.3$ Hz, 1H), 7.14 (dt, $J = 31.8, 7.9$ Hz, 3H), 6.51 (s, 1H), 4.27 (s, 2H), 3.61 (s, 3H). MS(ESI): 433.1 $[\text{M} + \text{H}]^+$; Anal. Calcd for $\text{C}_{24}\text{H}_{18}\text{F}_2\text{N}_4\text{S}$: C 66.65, H 4.20, N 12.95, found: C 66.66, H 4.19, N 12.93.

4.2.8 | 3-(5-([3-Chloro-4-fluorobenzyl]thio)-4-phenyl-4H-1,2,4-triazol-3-yl)-1-methyl-1H-indole (9)

Yellow powder, yield: 52.3%, m.p. $183\text{--}185^\circ\text{C}$; ^1H NMR (400 MHz, DMSO-d_6) δ : 8.15 (d, $J = 7.9$ Hz, 1H), 7.66–7.55 (m, 5H), 7.46 (d, $J = 8.2$ Hz, 1H), 7.42–7.33 (m, 3H), 7.25 (t, $J = 7.1$ Hz, 1H), 7.17 (t, $J = 7.9$ Hz, 1H), 6.51 (s, 1H), 4.37 (s, 2H), 3.63 (s, 3H). MS(ESI): 449.1 $[\text{M} + \text{H}]^+$; Anal. Calcd for $\text{C}_{24}\text{H}_{18}\text{ClFN}_4\text{S}$: C 64.21, H 4.04, N 12.48, found: C 64.20, H 4.03, N 12.49.

4.2.9 | 3-(5-([4-Methoxybenzyl]thio)-4-phenyl-4H-1,2,4-triazol-3-yl)-1-methyl-1H-indole (10)

Light yellow powder, yield: 69.1%, m.p. $155\text{--}157^\circ\text{C}$; ^1H NMR (400 MHz, DMSO-d_6) δ : 8.20 (d, $J = 8.0$ Hz, 1H), 7.87–7.70 (m, 2H),

7.50 (d, $J = 8.2$ Hz, 2H), 7.35 (dd, $J = 8.0, 1.3$ Hz, 2H), 7.24 (dd, $J = 17.1, 7.6$ Hz, 4H), 7.22–7.08 (m, 2H), 6.50 (s, 1H), 4.33 (s, 2H), 3.87 (s, 3H) 3.73 (s, 3H). MS(ESI): 427.2 [M + H]⁺; Anal. Calcd for C₂₅H₂₂N₄O₅: C 70.40, H 5.20, N 13.14, found: C 70.41, H 5.22, N 13.13.

4.2.10 | 3-(5-([3,5-Dimethoxybenzyl]thio)-4-phenyl-4H-1,2,4-triazol-3-yl)-1-methyl-1H-indole (11)

White powder, yield: 55.6%, m.p. 175–177°C; ¹H NMR (400 MHz, DMSO-*d*₆) δ : 7.95 (dt, $J = 7.9, 1.0$ Hz, 1H), 7.64–7.54 (m, 5H), 7.58–7.43 (m, 4H), 7.24 (ddd, $J = 8.3, 7.0, 1.3$ Hz, 1H), 7.12 (ddd, $J = 8.0, 7.0, 1.0$ Hz, 1H), 6.85 (s, 1H), 4.45 (s, 2H) 3.70 (s, 6H), 3.63 (s, 3H). MS(ESI): 457.2 [M + H]⁺; Anal. Calcd for C₂₆H₂₄N₄O₂S: C 68.40, H 5.30, N 12.27, found: C 68.38, H 5.30, N 12.28.

4.2.11 | 1-Methyl-3-(4-phenyl-5-([3,4,5-trimethoxybenzyl]thio)-4H-1,2,4-triazol-3-yl)-1H-indole (12)

Light yellow powder, yield: 66.3%, m.p. 189–190°C; ¹H NMR (600 MHz, DMSO-*d*₆) δ : 8.14 (d, $J = 8.0$ Hz, 1H), 7.61 (t, $J = 7.4$ Hz, 1H), 7.56 (t, $J = 7.6$ Hz, 2H), 7.46 (d, $J = 8.2$ Hz, 1H), 7.25 (dd, $J = 12.8, 7.3$ Hz, 3H), 7.17 (t, $J = 7.5$ Hz, 1H), 6.57 (s, 2H), 6.50 (s, 1H), 4.26 (s, 2H), 3.69 (s, 6H), 3.63 (d, $J = 3.8$ Hz, 6H). MS(ESI): 487.2 [M + H]⁺; Anal. Calcd for C₂₇H₂₆N₄O₃S: C 66.65, H 5.39, N 11.51, found: C 66.64, H 5.38, N 11.50.

4.2.12 | 3-(5-([2-Fluorobenzyl]thio)-4-phenyl-4H-1,2,4-triazol-3-yl)-1-methyl-1H-indole (13)

Yellow powder, yield 53.3%, m.p. 170–171°C; ¹H NMR (400 MHz, DMSO-*d*₆) δ : 8.17 (d, $J = 7.9$ Hz, 1H), 7.60 (dt, $J = 14.4, 6.9$ Hz, 3H), 7.50–7.38 (m, 2H), 7.34 (d, $J = 6.9$ Hz, 3H), 7.28–7.12 (m, 4H). 6.49 (s, 1H), 4.37 (s, 2H), 3.67 (s, 3H). MS(ESI): 415.1 [M + H]⁺; Anal. Calcd for C₂₄H₁₉FN₄S: C 69.54, H 4.62, N 13.52, found: C 69.53, H 4.63, N 13.54.

4.2.13 | 3-(5-([2-Chlorobenzyl]thio)-4-phenyl-4H-1,2,4-triazol-3-yl)-1-methyl-1H-indole (14)

Light yellow powder, yield: 36.4%, m.p. 162–164°C; ¹H NMR (400 MHz, DMSO-*d*₆) δ : 8.16 (d, $J = 7.9$ Hz, 1H), 7.59 (dt, $J = 14.4, 6.9$ Hz, 5H), 7.48 (dd, $J = 13.7, 7.6$ Hz, 4H), 7.36–7.21 (m, 2H), 7.17 (t, $J = 7.5$ Hz, 1H), 6.50 (s, 1H), 4.45 (s, 2H). 3.63 (s, 3H). MS(ESI): 431.1 [M + H]⁺; Anal. Calcd for C₂₄H₁₉ClN₄S: C 66.89, H 4.44, N 13.00, found: C 66.90, H 4.43, N 13.01.

4.2.14 | 3-(5-([2-Bromobenzyl]thio)-4-phenyl-4H-1,2,4-triazol-3-yl)-1-methyl-1H-indole (15)

Light yellow powder, yield: 41.8%, m.p. 160–161°C; ¹H NMR (400 MHz, DMSO-*d*₆) δ : 8.17 (d, $J = 7.9$ Hz, 1H), 7.65–7.54 (m, 4H), 7.50–7.38 (m, 2H), 7.34 (d, $J = 6.8$ Hz, 3H), 7.25 (t, $J = 7.6$ Hz, 1H), 7.24–7.10 (m, 2H), 6.50 (s, 1H), 4.38 (s, 2H), 3.62 (s, 3H). MS(ESI): 477.1 [M + H]⁺; Anal. Calcd for C₂₄H₁₉BrN₄S: C 60.64, H 4.03, N 11.79, found: C 60.63, H 4.02, N 11.80.

4.2.15 | 3-(5-([3-Fluorobenzyl]thio)-4-phenyl-4H-1,2,4-triazol-3-yl)-1-methyl-1H-indole (16)

Yellow powder, yield: 40.1%, m.p. 171–173°C; ¹H NMR (400 MHz, DMSO-*d*₆) δ : 8.16 (d, $J = 7.9$ Hz, 1H), 7.68–7.52 (m, 3H), 7.47 (d, $J = 8.1$ Hz, 1H), 7.46–7.30 (m, 3H), 7.34–7.06 (m, 5H), 6.51 (s, 1H), 4.39 (s, 2H), 3.63 (s, 3H). MS(ESI): 415.1 [M + H]⁺; Anal. Calcd for C₂₄H₁₉FN₄S: C 69.54, H 4.62, N 13.52, found: C 69.53, H 4.63, N 13.51.

4.2.16 | 3-(5-([3-Chlorobenzyl]thio)-4-phenyl-4H-1,2,4-triazol-3-yl)-1-methyl-1H-indole (17)

Light yellow powder, yield: 56.4%, m.p. 166–167°C; ¹H NMR (400 MHz, DMSO-*d*₆) δ : 8.15 (d, $J = 8.0$ Hz, 1H), 7.68–7.54 (m, 3H), 7.50–7.41 (m, 2H), 7.40–7.29 (m, 5H), 7.25 (s, 1H), 7.21 (dt, $J = 32.1, 7.2$ Hz, 1H), 6.50 (d, $J = 1.9$ Hz, 1H), 4.37 (d, $J = 1.9$ Hz, 2H), 3.62 (m, 3H). MS(ESI): 431.1 [M + H]⁺; Anal. Calcd for C₂₄H₁₉ClN₄S: C 66.89, H 4.44, N 13.00, found: C 66.88, H 4.43, N 13.01.

4.2.17 | 3-(5-([3-Bromobenzyl]thio)-4-phenyl-4H-1,2,4-triazol-3-yl)-1-methyl-1H-indole (18)

White powder, yield: 47.7%, m.p. 164–166°C; ¹H NMR (400 MHz, DMSO-*d*₆) δ : 8.76 (s, 1H), 7.95 (dd, $J = 8.0, 1.1$ Hz, 1H), 7.66–7.54 (m, 3H), 7.58–7.41 (m, 3H), 7.24 (d, $J = 7.0$ Hz, 2H), 7.12 (dt, $J = 7.5, 7.0, 1.1$ Hz, 3H), 6.85 (s, 1H), 4.46 (s, 2H), 3.70 (s, 3H). MS(ESI): 477.1 [M + H]⁺; Anal. Calcd for C₂₄H₁₉BrN₄S: C 60.64, H 4.03, N 11.79, found: C 60.65, H 4.04, N 11.81.

4.2.18 | 3-(5-([4-Fluorobenzyl]thio)-4-phenyl-4H-1,2,4-triazol-3-yl)-1-methyl-1H-indole (19)

Yellow powder, yield: 46.7%, m.p. 169–170°C; ¹H NMR (400 MHz, DMSO-*d*₆) δ : 8.18 (d, $J = 7.9$ Hz, 1H), 7.61–7.55 (m, 3H), 7.50–7.38 (m, 2H), 7.34 (d, $J = 6.9$ Hz, 3H), 7.23–7.09 (m, 4H). 6.52 (s, 1H), 4.40 (s, 2H), 3.61 (s, 3H). MS(ESI): 415.1 [M + H]⁺; Anal. Calcd for C₂₄H₁₉FN₄S: C 69.54, H 4.62, N 13.52, found: C 69.53, H 4.63, N 13.51.

4.2.19 | 3-(5-([4-Chlorobenzyl]thio)-4-phenyl-4H-1,2,4-triazol-3-yl)-1-methyl-1H-indole (20)

Light yellow powder, yield: 36.4%, m.p. 165–167°C; ^1H NMR (400 MHz, DMSO- d_6) δ : 8.16 (d, J = 8.0 Hz, 1H), 7.68–7.55 (m, 3H), 7.49 (dd, J = 18.3, 8.3 Hz, 3H), 7.35 (dd, J = 13.1, 7.6 Hz, 4H), 7.25 (t, J = 7.0 Hz, 1H), 7.17 (t, J = 7.5 Hz, 1H), 6.50 (s, 1H), 4.35 (s, 2H), 3.63 (s, 3H). MS(ESI): 449.1 [M + H] $^+$; Anal. Calcd for $\text{C}_{24}\text{H}_{19}\text{ClN}_4\text{S}$: C 66.89, H 4.44, N 13.00, found: C 66.87, H 4.45, N 12.99.

4.2.20 | 3-(5-([4-Bromobenzyl]thio)-4-phenyl-4H-1,2,4-triazol-3-yl)-1-methyl-1H-indole (21)

White powder, yield: 55.1%, m.p. 161–162°C; ^1H NMR (400 MHz, DMSO- d_6) δ : 8.15 (d, J = 7.8 Hz, 1H), 7.68–7.55 (m, 4H), 7.49 (dd, J = 18.1, 8.3 Hz, 3H), 7.35 (dd, J = 13.0, 7.6 Hz, 3H), 7.21 (dt, J = 32.7, 7.0 Hz, 2H), 6.55 (s, 1H), 4.46 4.35 (s, 2H), 3.63 (s, 3H). MS(ESI): 477.1 [M + H] $^+$; Anal. Calcd for $\text{C}_{24}\text{H}_{19}\text{BrN}_4\text{S}$: C 60.64, H 4.03, N 11.79, found: C 60.63, H 4.04, N 11.80.

4.2.21 | 3-(5-([4-Iodobenzyl]thio)-4-phenyl-4H-1,2,4-triazol-3-yl)-1-methyl-1H-indole (22)

Yellow powder, yield: 40.7%, m.p. 197–199°C; ^1H NMR (400 MHz, DMSO- d_6) δ : 8.15 (d, J = 7.9 Hz, 1H), 7.71–7.55 (m, 6H), 7.46 (d, J = 8.1 Hz, 1H), 7.36 (d, J = 6.8 Hz, 2H), 7.25 (t, J = 7.0 Hz, 1H), 7.18 (d, J = 8.3 Hz, 2H), 6.50 (s, 1H), 4.33 (s, 2H), 3.63 (s, 3H). MS(ESI): 523.0 [M + H] $^+$; Anal. Calcd for $\text{C}_{24}\text{H}_{19}\text{IN}_4\text{S}$: C 55.18, H 3.67, N 10.72, found: C 55.19, H 3.66, N 10.71.

4.2.22 | 1-Methyl-3-(5-([4-methylbenzyl]thio)-4-phenyl-4H-1,2,4-triazol-3-yl)-1H-indole (23)

Light yellow powder, yield: 69.1%, m.p. 155–157°C; ^1H NMR (400 MHz, DMSO- d_6) δ : 8.16 (d, J = 7.9 Hz, 1H), 7.67–7.54 (m, 3H), 7.46 (d, J = 8.2 Hz, 1H), 7.33 (dd, J = 8.0, 1.3 Hz, 2H), 7.24 (dd, J = 17.1, 7.6 Hz, 3H), 7.22–7.08 (m, 3H), 6.50 (s, 1H), 4.33 (s, 2H), 3.63 (s, 3H), 2.27 (s, 3H). MS(ESI): 411.2 [M + H] $^+$; Anal. Calcd for $\text{C}_{25}\text{H}_{22}\text{N}_4\text{S}$: C 73.14, H 5.40, N 13.65, found: C 73.13, H 5.42, N 13.66.

4.2.23 | 1-Methyl-3-(4-phenyl-5-([4-(trifluoromethyl)benzyl]thio)-4H-1,2,4-triazol-3-yl)-1H-indole (24)

Light yellow powder, yield: 47.3%, m.p. 178–179°C; ^1H NMR (400 MHz, DMSO- d_6) δ : 7.73 (s, 1H), 7.60 (dd, J = 23.2, 9.2 Hz, 7H), 7.46 (d, J = 8.1 Hz, 1H), 7.31 (d, J = 7.6 Hz, 2H), 7.29–7.14 (m, 2H), 6.49 (s, 1H), 4.46 (s, 2H), 3.36 (s, 3H). MS(ESI): 465.1 [M + H] $^+$; Anal.

Calcd for $\text{C}_{25}\text{H}_{19}\text{F}_3\text{N}_4\text{S}$: C 60.64, H 4.12, N 12.06, found: C 60.65, H 4.13, N 12.04.

4.3 | Cell culture

Human hepatoma cell (HepG2), carcinoma of cervix cell (HeLa), human breast cancer cells (MCF-7), human lung adenocarcinoma cells (A549), and human renal epithelial cells (293T) were maintained in DMEM (Dulbecco's modified Eagle's medium) with 1% antibiotic (100 U/ml penicillin and 100 $\mu\text{g}/\text{ml}$ streptomycin) and 10% FBS (fetal bovine serum) in a humidified atmosphere in 5% CO_2 at 37°C.

4.4 | Antiproliferation assay

According to the previous reports (Tsyganov et al., 2013; Zheng et al., 2014), target tumor cells were grown to log phase in DMEM medium supplemented with 10% FBS. After reaching a dilution of 10^5 cells ml^{-1} with the medium, 100 μl of the obtained cell suspension was added to each well of 96-well culture plates and then incubation was performed at 37°C in 5% CO_2 atmosphere for 12 h before being subjected to antiproliferation assessment. Tested samples at preset concentrations (0.1, 1, 10, and 100 μM) were added to 96 wells with colchicine as positive reference. After a 24 h exposure period, 25 ml of PBS containing 2.5 mg/ml of MTT was added to each well, and the cells were incubated at 37°C for 4 h. Then, the solution was poured out and 150 μl DMSO was added to dissolve the purple formazan crystals produced. The optical absorbance was measured at 570 nm. Each assay was carried out for at least three times.

4.5 | Tubulin polymerization assay

According to the previous reports (Yang et al., 2019; Yang et al., 2020), bovine brain tubulin was purified as described previously. To evaluate the effect on tubulin assembly in vitro, various concentrations of the compounds (6–24) were preincubated with 10 μM tubulin in glutamate buffer at 30°C to 0°C. And then the addition of GTP, the mixtures were transferred to cuvettes at 0°C in a recording spectrophotometer and warmed up to 30°C. The IC_{50} was defined as the compound concentration that inhibited the extent of assembly by 50% after 20 min incubation. In all experiments three replicate wells were used for each drug concentration.

4.6 | In vitro cytotoxicity test of 293T

In this study, the cytotoxic activity in vitro was measured using the MTT assay. It is generally known that the human renal epithelial cells (293T) was used to test the toxicity of compounds. The prepared suspension was added into the 96-well plates to be incubated for about 12 h. Subsequently various concentrations of the test compounds

(0.1, 1, 10, and 100 μM) were added to the per well and grown at 37°C for 24 h. And then 5 mg/ml of MTT (20 μl) was added each well 4 h before the termination of the incubation. After the supernatant was removed, 150 μl DMSO was added to dissolve the formazan crystals. The absorbance was read at a wavelength of 570 nm. Each assay was replicated for three times.

4.7 | Cell apoptosis assay

Approximately 10^5 cells/well were seeded in a 6-well plate and allowed to adhere. The medium was replaced with fresh culture medium containing compound **12** at final concentrations of 0, 0.1, 0.15, and 0.2 μM . After 24 h, cells were trypsinized, washed twice with PBS, subsequently centrifuged (1500 rpm at 4°C for 5 min) and stained with 5 μl of Annexin V-FITC and 5 μl of PI in binding buffer for 15 min at room temperature (25°C) in the dark. In the test, about 10,000 cells were counted. Apoptosis analysis was performed using a FACScaliber (FACScan; BD Biosciences) equipped with a CellQuest software (BD Biosciences).

4.8 | Cell cycle analysis

About 5×10^5 cells/well were plated in 6-well plates and incubated at 37°C for 24 h to adhere. The medium was then washed off and fresh culture medium containing 0, 0.1, 0.15, and 0.2 μM compound **12** was added. After the incubation, the cells were collected, centrifuged, fixed overnight at 4°C with ice-cold 70% ethanol. The next day ethanol was removed, and the cells were in PBS (phosphate buffered saline) containing stained with 0.1 mg/ml of RNase, 5 $\mu\text{g/ml}$ PI and stained at 37°C for 30 min, and then subjected to flow cytometric analysis. The percentage of cells in the G1, S, and G2/M phases of the cell cycle were determined with Flowjo 7.6.1 software.

4.9 | Western blot analysis

HeLa cells were incubated in the presence of compound **12**. After 24 h, the cells were collected, centrifuged, and washed twice with ice-cold PBS (phosphate buffered saline) and the pellet was lysed in RIPA lysis buffer (50 mM Tris-HCl, 150 mM NaCl, 0.1% SDS, 1% NP-40, 0.25% Sodium deoxycholate, and 1 mM EDTA, pH 8.0) with freshly added protease inhibitor cocktail (Roche) on ice for 30 min, and then centrifuged at 15,000g at 4°C for 10 min. The supernatant was collected, and the protein concentration was calculated with a BCA protein assay kit (Thermo Scientific, Rockford, Illinois). The proteins were separated via SDS-PAGE (Bio-Rad), and boiled at 100°C for 5 min. After electrophoresis, the proteins were electrotransferred to PVDF membranes (Bio-Rad) and then blocked with 5% skim milk at room temperature for 2 h. Membranes were incubated with primary antibodies against Cyclin B1 (Cell Signaling), p-cdc2Tyr15 (Cell Signaling), Bcl-2, Bcl-x1 (Millipore), and β -actin (Sigma-Aldrich) overnight at 4°C.

After being washed three times in TBST, the membranes were incubated with the suitable HRP-conjugated secondary antibodies for 2 h at room temperature. Follow by three additional washes with TBST, the membranes were detected with the SuperSignal West Pico chemiluminescence substrate (Abcam) and imaged by darkroom exposure.

4.10 | Docking simulations

The 3D X-ray structure of tubulin (PDB code: 4O2B) was chosen as the template for the modeling study of compound **12**. The crystal structures of tubulin domain bound to colchicine were retrieved from the RCSB Protein Data Bank (<http://www.rcsb.org/pdb/home/home.do>). Molecular docking was carried out using the Discovery Studio (version 3.5) as implemented through the graphical user interface DS-CDOCKER protocol consulting the references (Li, Pan, et al., 2020a; Li, Wu, et al., 2020b; Pan et al., 2020). The synthesized compounds **6–24** were constructed using Chem. 3D ultra 14.0 software. All bound water and ligands were eliminated from the protein and the polar hydrogen was added. The whole tubulin complex was defined as a receptor and the site sphere was selected based on the ligand binding location of colchicine (LOC503), then the LOC503 molecule was removed and replaced by compound **12** during the molecular docking procedure. All the types of the interactions of the docked protein with ligand were analyzed at the end of molecular docking.

ACKNOWLEDGMENTS

This research was funded by Natural Science Foundation of Guangxi Province under Grant No.2019AC20294, Guangxi University for Nationalities Research Funded Project (No. 2018KJQD13) and Guangxi biological polysaccharide separation, purification and modification research platform (GKZY18076005). Dr. H.L. Zhu thanks for the support of Lianyungang talent project.

CONFLICT OF INTEREST

The authors declare no conflicts of interest.

DATA AVAILABILITY STATEMENT

The data that support the findings of this study are available on request from the corresponding author. The data are not publicly available due to privacy or ethical restrictions.

ORCID

Ruo-Jun Man  <https://orcid.org/0000-0001-5434-4229>

REFERENCES

- Amos, L. A. (2004). Microtubule structure and its stabilisation. *Organic & Biomolecular Chemistry*, 2, 2153–2160.
- Alhamadsheh, M. M., Musayev, F., Komissarov, A. A., Sachdeva, S., Wright, H. T., Scarsdale, N., Florova, G., & Reynolds, K. A. (2007). Alkyl-CoA disulfides as inhibitors and mechanistic probes for FabH enzymes. *Chemistry & Biology*, 14, 513–524.
- Brennan, C. W., Verhaak, R. G. W., McKenna, A., Campos, B., Nounshmehr, H., Salama, S. R., Zheng, S., Chakravarty, D.,

- Sanborn, J. Z., Berman, S. H., Beroukhir, R., Bernard, B., Wu, C. J., Genovese, G., Shmulevich, I., Barnholtz-Sloan, J., Zou, L., Vegesna, R., Shukla, S. A., ... McLendon, R. (2013). The somatic genomic landscape of Glioblastoma. *Cell*, 155, 462–477.
- Campbell, J. W., & Cronan, J. E. (2001). Bacterial fatty acid biosynthesis: Targets for antibacterial drug discovery. *Annual Review of Microbiology*, 55, 305–332.
- Dumontet, C., & Jordan, M. A. (2010). Microtubule-binding agents: A dynamic field of cancer therapeutics. *Nature Reviews Drug Discovery*, 9, 790–803.
- Flynn, B. L., Gill, G. S., Grobelny, D. W., Chaplin, J. H., Paul, D., Leske, A. F., Lavranos, T. C., Chalmers, D. K., Charman, S. A., Kostewicz, E., Shackelford, D. M., Morizzi, J., Hamel, E., Jung, M. K., & Kremmidiotis, G. (2011). Discovery of 7-hydroxy-6-methoxy-2-methyl-3-(3,4,5-trimethoxybenzoyl)benzo[b]furan(BNC105), a tubulin polymerization inhibitor with potent antiproliferative and tumor vascular disrupting properties. *Journal of Medicinal Chemistry*, 54, 6014–6027.
- Gan, H. K., Cvriljevic, A. N., & Johns, T. G. (2013). The epidermal growth factor receptor variant III (EGFRvIII): Where wild things are altered. *FEBS Journal*, 280, 5350–5370.
- Honore, S., Pasquier, E., & Braguer, D. (2005). Understanding microtubule dynamics for improved cancer therapy. *Cellular and Molecular Life Sciences*, 62, 3039–3056.
- Jordan, M. A., & Wilson, L. (2004). Microtubules as a target for anticancer drugs. *Nature Reviews Cancer*, 4, 253–265.
- Kamal, A., Kumar, G. B., Polepalli, S., Shaik, A. B., Reddy, V. S., Reddy, M. K., Reddy, C. R., Mahesh, R., Kapure, J. S., & Jain, N. (2014a). Design and synthesis of aminostilbene-arylpropenones as tubulin polymerization inhibitors. *ChemMedChem*, 9, 2565–2579.
- Kamal, A., Reddy, V. S., Santosh, K., Kumar, G. B., Shaik, A. B., Mahesh, R., Chourasiya, S. S., Sayeed, I. B., & Kotamraju, S. (2014b). Synthesis of imidazo[2,1-b][1,3,4]thiadiazole-chalcones as apoptosis inducing anticancer agents. *MedChemComm*, 5, 1718–1723.
- Kavallaris, M., Verrills, N. M., & Hill, B. T. (2001). Anticancer therapy with novel tubulin-interacting drugs. *Drug Resistance Updates*, 4, 392–401.
- Li, D. D., Pan, Y., Jiang, Y., Wang, Z. Z., Xiao, W., & Zhao, L. G. (2020a). Molecular insights into catalytic specificity of α -L-rhamnosidase from *Bacteroides thetaiotaomicron* by molecular docking and dynamics. *Chemical Physics Letters*, 754, 137695.
- Li, D. D., Wu, T. T., Pan, Y., Wang, Z. Z., Xiao, W., Jiang, Y., & Zhao, L. G. (2020b). Molecular dynamics analysis of binding sites of epidermal growth factor receptor kinase inhibitors. *ACS Omega*, 5, 16307–16314.
- Li, H. Q., Luo, Y., & Zhu, H. L. (2011a). Discovery of vinylogous carbamates as a novel class of β -ketoacyl-acyl carrier protein synthase III (FabH) inhibitors. *Bioorganic & Medicinal Chemistry*, 19, 4454–4459.
- Li, Z. L., Li, Q. S., Zhang, H. J., Hu, Y., Zhu, D. D., & Zhu, H. L. (2011b). Design, synthesis and biological evaluation of urea derivatives from *o*-hydroxybenzylamines and phenylisocyanate as potential FabH inhibitors. *Bioorganic & Medicinal Chemistry*, 19, 4413–4420.
- Mahindroo, N., Liou, J. P., Chang, J. Y., & Hsieh, H. P. (2006). Antitubulin agents for the treatment of cancer—a medicinal chemistry update. *Expert Opinion on Therapeutic Patents*, 16, 647–691.
- McIntosh, J. R., Grishchuk, E. L., & West, R. R. (2002). Chromosome-microtubule interactions during mitosis. *Annual Review of Cell and Developmental Biology*, 18, 193–219.
- Meng, J. P., Geng, R. X., Zhou, C. H., & Gan, L. L. (2009). Advances in the research of benzimidazole drugs. *Chinese Journal of New Drugs and Clinical Remedies*, 18, 1505–1514.
- Nakagawa-Goto, K., Wu, P. C., Lai, C. Y., Hamel, E., Zhu, H., Zhang, L., Kozaka, T., Ohkoshi, E., Goto, M., Bastow, K. F., & Lee, K. H. (2011). Antitumor agents. 284. New Desmosmumotin B analogues with bicyclic B-ring as cytotoxic and antitubulin agents. *Journal of Medicinal Chemistry*, 54, 1244–1255.
- Pan, Y., Li, D. D., Wang, L., Zhang, L. H., Cao, F. L., Fang, X. Y., & Zhao, L. G. (2020). Identification of dihydroorotate dehydrogenase as a protein target of ginkgolic acid by molecular docking and dynamics. *Journal of Molecular Structure*, 1220, 128692.
- Pettit, G., Lippert, J., Boyd, M., Verdier-Pinard, P., & Hamel, E. (2000). Antineoplastic agents 442. Synthesis and biological activities of diroxostatin. *Anti-Cancer Drug Design*, 15, 361–371.
- Pettit, G., & Rhodes, M. (1998). Antineoplastic agents 389. New syntheses of the combretastatin A-4 prodrug. *Anti-Cancer Drug Design*, 13, 183–191.
- Prota, A. E., Danel, F., Bachmann, F., Bargsten, K., Buey, R. M., Pohlmann, J., Reinelt, S., Lane, H., & Steinmetz, M. O. (2014). The novel microtubule-destabilizing drug BAL27862 binds to the colchicine site of tubulin with distinct effects on microtubule organization. *Journal of Molecular Biology*, 426, 1848–1860.
- Ravelli, R. B. G., Gigant, B., Curmi, P. A., Jourdain, I., Lachkar, S., Sobel, A., & Knossow, M. (2004). Insight into tubulin regulation from a complex with colchicine and a stathmin-like domain. *Nature*, 428, 198–202.
- Risinger, A. L., Giles, F. J., & Mooberry, S. L. (2009). Microtubule dynamics as a target in oncology. *Cancer Treatment Reviews*, 35, 255–261.
- Rustin, G. J., Shreeves, G., Nathan, P. D., Gaya, A., Ganesan, T. S., Wang, D., Boxall, J., Poupard, L., Chaplin, D. J., Stratford, M. R. L., Balkissoon, J., & Zweifel, M. (2010). A phase Ib trial of CA4P (combretastatin A-4 phosphate), carboplatin and paclitaxel in patients with advanced cancer. *British Journal of Cancer*, 102, 1355–1360.
- Sharma, S., Poliks, B., Chiauzzi, C., Ravindra, R., Blanden, A. R., & Bane, S. (2010). Characterization of the colchicine binding site on avian tubulin isotype β VI. *Biochemistry*, 49, 2932–2942.
- Solum, E. J., Cheng, J. J., Sørvik, I. B., Paulsen, R. E., Vik, A., & Hansen, T. V. (2014). Synthesis and biological evaluations of new analogs of 2-methoxyestradiol: Inhibitors of tubulin and angiogenesis. *European Journal of Medicinal Chemistry*, 85, 391–398.
- Szczepankiewicz, B. G., Liu, G., Jae, H. S., Tasker, A. S., Gunawardana, I. W., von Geldern, T. W., Gwaltney, S. L., Wu-Wong, J. R., Gehrke, L., Chiou, W. J., Credo, R. B., Alder, J. D., Nukkala, M. A., Zielinski, N. A., Jarvis, K., Mollison, K. W., Frost, D. J., Bauch, J. L., Hui, Y. H., ... Rosenberg, S. H. (2001). New antimetabolic agents with activity in multi-drug-resistant cell lines and in vivo efficacy in murine tumor models. *Journal of Medicinal Chemistry*, 44, 4416–4430.
- Tanitime, A., Oyamada, Y., Ofuji, K., Fujimoto, M., Iwai, N., Hiyama, Y., Suzuki, K., Ito, H., Terauchi, H., Kawasaki, M., Nagai, K., Wachi, M., & Yamagishi, J. I. (2004). Synthesis and antibacterial activity of a novel series of potent DNA gyrase inhibitors, Pyrazole derivatives. *Journal of Medicinal Chemistry*, 47, 3693–3696.
- Teicher, B. A. (2008). Newer cytotoxic agents: Attacking cancer broadly. *Clinical Cancer Research*, 14, 1610–1617.
- Tsyganov, D. V., Konyushkin, L. D., Karmanova, I. B., Firgang, S. I., Strelenko, Y. A., Semenova, M. N., Kiselyov, A. S., & Semenov, V. V. (2013). Cis-restricted 3-aminopyrazole analogues of combretastatins: Synthesis from plant polyalkoxybenzenes and biological evaluation in the cytotoxicity and phenotypic sea urchin embryo assays. *Journal of Natural Products*, 76, 1485–1491.
- Walczak, C. E. (2000). Microtubule dynamics and tubulin interacting proteins. *Current Opinion in Cell Biology*, 12, 52–56.
- Yang, F., Yu, L. Z., Diao, P. C., Jian, X. E., Zhou, M. F., Jiang, C. S., You, W. W., Ma, W. F., & Zhao, P. L. (2019). Novel [1,2,4]triazolo [1,5- α]pyrimidine derivatives as potent antitubulin agents: Design, multicomponent synthesis and antiproliferative activities. *Bioorganic Chemistry*, 92, 103260.
- Yang, F., Jian, X. E., Diao, P. C., Huo, X. S., You, W. W., & Zhao, P. L. (2020). Synthesis, and biological evaluation of 3,6-diaryl-[1,2,4]triazolo [4,3-a]pyridine analogues as new potent tubulin polymerization inhibitors. *European Journal of Medicinal Chemistry*, 204, 112625.

- Yu, K., Li, R., Yang, Z., Wang, F., Wu, W. S., Wang, X. Y., Nie, C. L., & Chen, L. J. (2015). Discovery of a potent microtubule-targeting agent: Synthesis and biological evaluation of water-soluble amino acid prodrug of combretastatin A-4 derivatives. *Bioorganic & Medicinal Chemistry Letters*, *25*, 2302–2307.
- Zheng, S., Zhong, Q., Mottamal, M., Zhang, Q., Zhang, C., Lemelle, E., McFerrin, H., & Wang, G. (2014). Design, synthesis, and biological evaluation of novel pyridine-bridged analogues of combretastatin-A4 as anticancer agents. *Journal of Medicinal Chemistry*, *57*, 3369–3381.
- Zhou, J., & Giannakakou, P. (2005). Targeting microtubules for cancer chemotherapy. *Current Medicinal Chemistry*, *5*, 65–71.
- Zweifel, M., Jayson, G. C., Reed, N. S., Osborne, R., Hassan, B., Ledermann, J., Shreeves, G., Poupard, L., Lu, S. P., Balkissoon, J., Chaplin, D. J., & Rustin, G. J. S. (2011). Phase II trial of combretastatin

A4 phosphate, carboplatin, and paclitaxel in patients with platinum-resistant ovarian cancer. *Annals of Oncology*, *22*, 2036–2041.

SUPPORTING INFORMATION

Additional supporting information may be found online in the Supporting Information section at the end of this article.

How to cite this article: Wu M-K, Man R-J, Liao Y-J, Zhu H-L, Zhou Z-G. Discovery of novel indole-1,2,4-triazole derivatives as tubulin polymerization inhibitors. *Drug Dev Res.* 2021;1–13. <https://doi.org/10.1002/ddr.21805>